*Research Article*

# Study on Pretightening Loss Effect of Bolt Support in Deep Soft Rock Roadway

**Fenghai Yu,[1,2] Bo Sun [1,2] Qingduo Wang,[1,2] Ping Fang,[3] Tao Zhang,[3] Jianchong Chen,[3] Xin Zhao,[3] and Dehe Zhu[3]**

[1]*College of Energy and Mining Engineering, Shandong University of Science and Technology, Qingdao 266590, China*
[2]*State Key Laboratory of Mining Disaster Prevention and Control, Shandong University of Science and Technology,*
 *Qingdao 266590, China*
[3]*Ordos Haohua Hongqingliang Mining Co., Ltd, Ordos 014300, China*

Correspondence should be addressed to Bo Sun; 202183010033@sdust.edu.cn

The magnitude of pretension force serves as an important indicator of the effectiveness of anchor bolt active support and is one of the significant factors influencing the stability of tunnel surrounding rock. Therefore, in practical engineering, it is crucial to establish the relationship between pretension torque and pretension force. However, current research in this field has some limitations. With a specific mine in western China as the engineering background, this paper first analyzed the influence factors of surrounding rock deformation and failure, established a mechanical model for pretension structure of anchor bolt support, and derived the quantitative relationship between pretension torque and pretension force based on hypothetical conditions. Finally, it proposed the loss effect of anchor bolt support and modified the pretightening loss coefficient for engineering application. The research results show that the actual pretightening force of anchor support is lower due to the influence of deep soft coal seam, which leads to failure of coal pillar under mining stress. The loss effect of surrounding rock on pretightening force was represented by a coefficient $k$, and the modified value of the coefficient was calculated as 0.19~0.43. By applying the modified relationship between pretightening torque and pretightening force, it was found that the actual pretightening torque of 300 Nm applied to 11307 return air roadway effectively controlled surrounding rock deformation and failure, with coal pillar displacement less than 120 mm.

## 1. Introduction

With the gradual depletion of resources in the shallow mining areas in the east, the focus of coal mining gradually extends deep and develops to the western mining areas. Weak coal rock is widely distributed in the western mining area, which has the characteristics of low strength, large plasticity, and easy breakage [1–3]. After the excavation of deep soft coal roadway, the deformation speed of surrounding rock is fast, the damage range is large, the initial support resistance of roadway is small, and it is difficult to effectively control the deformation of surrounding rock of the roadway.

Aiming at the problem of insufficient initial support strength of roadway, Sun et al. [4] systematically revealed the instability mechanism of deep coal roadway and provided some schemes to maintain the stability of roadway, which can significantly promote the sustainable development of mining industry. They analyzed the mechanical properties and supporting mechanism of bolt [5] and developed various forms of bolt [6, 7], high prestressed bolt, and other supporting methods [8, 9] and control methods of surrounding rock deformation [10]. Through field research, it was found that when the bolt support resistance reached more than 40 kN, the roadway deformation could be effectively controlled [11]. However, it also faces some severe

challenges [12]. As an important parameter of bolt support, pretightening force plays an important role in controlling roadway deformation [13–16]. For the study of the effect of bolt pretightening force support, scholars analyzed the stress field distribution characteristics of surrounding rock under different pretightening forces through numerical comparison experiments and proposed that improving the pretightening force of bolt can effectively improve the stiffness of anchor body [17, 18] and strengthen the antidynamic load impact performance of anchor body [19–21]. Guo et al. [22, 23] studied the effect of roadway support during mining and used the statistical analysis theory and exponential function to express the convergence model to simulate the stress characteristics of the main roadway. Hyett et al. [24] studied the bearing capacity of rod bodies with different lengths under different rock conditions through indoor experiments. Kang [25] introduced the case study of the bolt support system for soft rock reinforcement, which is helpful to improve the engineering application of bolt support in long-wall roadway excavated in soft rock mass. Ru and Wenkai [26] took Gaojialiang Coal Mine in western China as the research object and studied the failure mechanism of roadway roof under residual coal pillars in shallow and close multiseam combined with field monitoring and numerical simulation. In order to evaluate the design of roadway bolt support, Zhang [27] carried out bolt stress monitoring on several sections of roadway during roadway excavation and studied the parameters of anchorage length and bolt spacing by the numerical model. The pretightening force of the bolt is generated by applying the pretightening torque. For this reason, scholars have established the mechanical model of the bolt, analyzed the influencing factors between the pretightening force and the pretightening torque of the bolt, obtained the theoretical relationship between the pretightening force and the pretightening torque, and verified the accuracy of the relationship in the laboratory test [28]. In practical engineering, the pretightening force of bolt is affected by many factors. Aiming at the problem of conversion efficiency between pretightening force and torque of bolt, scholars [29–32] have carried out experimental research on different thread parameters of bolt tail, obtained the relationship between different thread structure parameters and mechanical properties of bolt thread section, and put forward the control measures of pretightening force of bolt in coal mine. Experts and scholars [33–37] provide experience for this study through numerical simulation research and analysis. At present, there are many studies on the relationship between the bolt preload and preload torque. Tian et al. [38] proposed a method to identify the stiffness parameters of bolt connection related to preload torque. Afzali et al. [39] believe that in terms of preload loss, the preload loss of pretightened stainless steel bolt connection is similar to that of carbon steel connection because their preload loss is equivalent. However, there is a loss in the pretightening force of the bolt during the on-site construction process, which makes the actual pretightening force deviate from the theoretical pretightening force. The

initial support resistance of the bolt is insufficient, and its support effect has not been fully utilized. The quantitative relationship between the bolt pretightening force and the pretightening torque under the condition of deep soft coal roadway needs to be further studied.

In this paper, field investigation, laboratory test, theoretical analysis, numerical simulation, and field test are used to study and obtain the deformation characteristics of the roadway side, analyze the causes of roadway side deformation, establish a mechanical model to derive the relationship between pretightening force and pretightening torque, and obtain the relationship between actual pretightening force and pretightening torque of deep soft rock roadway through field test. The theoretical value is corrected to determine the pretightening torque value required by the design pretightening force corresponding to the field, and the field application test is carried out.

## 2. Deformation Failure Analysis of Deep Weak Coal

*2.1. Engineering Geology.* Hongqingliang Coal Mine mainly mines 3-1 coal seam at present. The buried depth of the mining coal seam is 467~533 m, and the inclination angle of the mining coal seam is 0~6°. The coal seam structure is relatively simple and stable, and the endogenous fissures are more developed. The hydrogeological conditions of the mine are simple, and there is water leaching in some areas. At present, the roadway of 11307 working face of 3-1 coal seam is excavated. Four months after the end of the mining of the 11302 working face adjacent to the south, the 11307 return airway began to be dug. The 11307 return air roadway is 50 m away from the goaf of 11302 working face, and the northern working face has not started mining. The relationship between each working face and roadway is shown in Figure 1.

The coal seam thickness of 11307 working face is 2.1~6.3 m, with an average of 4.3 m. The roof is mainly sandy mudstone and conglomerate, and the floor is mainly sandy mudstone and siltstone. The maximum uniaxial compressive strength of coal measured in the borehole of underground roadway is 18.5 MPa, and the uniaxial compressive strength of sandy mudstone is concentrated in 14.3~27.2 MPa. The lithology of roof and floor in the excavation stage of 11307 working face is shown in Table 1.

*2.2. Support Condition.* The 11307 tail entry is 5.0 m wide and 3.6 m high, with "anchor-net-cable" support. The anchor rod mainly adopts $\varphi 22 \times 2600$ mm deformed steel fine wire anchor rod with a row spacing of $700 \times 1000$ mm; the row spacing between roadway sides is $800 \times 1000$ mm and tray is $200 \times 200 \times 10$ mm dish tray. The anchor cable mainly adopts $\varphi 21.8 \times 7300$ mm high-strength shear anchor cable, arranged in 3-3-3, with spacing of $1500 \times 2000$ mm. The bolt pretightening force is designed to be 60 kN, and the applied pretightening torque is designed to be 240 N·m. The specific support section is shown in Figure 2.
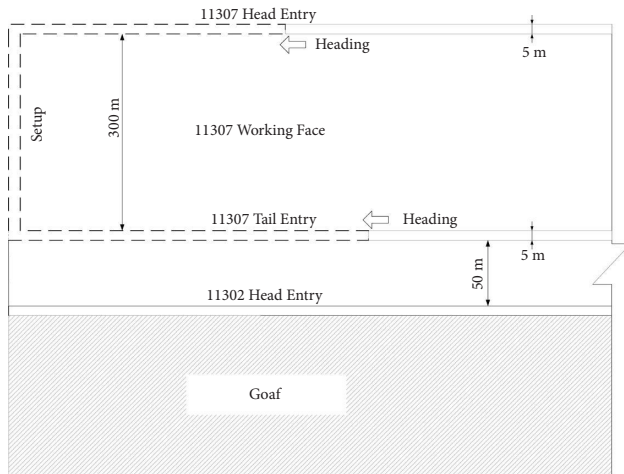
Figure 1: Excavation diagram of 11307 working face.

### 2.3. Deformation and Failure Characteristics of the Return Airway Wall

#### 2.3.1. Overall Failure Characteristics.
The roof and floor of 11307 return air roadway are mainly sandy mudstone or siltstone with low strength, with well-developed bedding and poor cementation between layers. As shown in Figure 3, the overall deformation and failure of the roadway after a period of time is more serious, which are manifested as follows:

(1) The overall subsidence of the roof is fast and the subsidence is large, about 372 mm. The subsidence of the local severe area can reach 454 mm, and the coal body is broken.

(2) The two sides have a large amount of drum, and the gob side is particularly serious. The maximum displacement can reach 353 mm. The deformation of the side mesh is more serious, the deformation of the mining side is relatively small, and the displacement reaches 114 mm.

(3) The amount of floor heave is about 196 mm, and the cracking of the floor in some areas is serious, up to 500 mm.

#### 2.3.2. Monitoring and Analysis of the Roadway Mine Pressure Law.
During the excavation of 11307 return air roadway, a group of measuring points are set every 100 m, and a total of 5 groups are arranged to measure the deformation of roof and floor, gob side, mining side, and bolt working resistance, respectively. The average displacement of monitoring results and the working resistance curve of bolt are shown in Figure 4.

(1) The overall surrounding rock of the roof, floor, and mining side is relatively complete, and the displacement is relatively small. After the roadway is excavated for 45 m, the deformation of both sides is basically stable, and the displacement is 130 and 85 mm, respectively. The deformation along the goaf is far greater than that of the roof, floor, and mining side, and after the latter tends to be stable, the deformation along the goaf still continues. After the roadway is excavated for 70 m, the deformation along the goaf basically tends to be stable, and the displacement reaches 350 mm.

(2) After the bolt is installed and the design pretightening torque is applied, the pretightening force along the goaf side and the mining side are 35 kN and 42 kN, respectively. With the increase of the advance distance, the working resistance of the goaf side bolt is gradually increased. The working resistance of the goaf side bolt is less than the mining side. After 40 m of roadway excavation, the working resistance of the mining side bolt basically tends to be stable, with the size of 103 kN. At this time, the supporting resistance of the goaf side bolt continues to rise and tends to be stable after 80 m of roadway excavation, with the size of 116 kN.

### 2.4. Analysis of Influencing Factors of Deformation and Failure of Roadway Surrounding Rock.
Based on the above-mentioned summary and analysis of the destruction characteristics of the 11307 tail entry in Hongqingliang Coal Mine, it is concluded that the deformation causes of the 11307 tail entry are as follows:

(1) The surrounding rock strength of roadway is low. Hongqingliang Coal Mine belongs to deep soft rock roadway, which has broken coal and rock mass, low strength, and developed joints. In the process of roadway excavation, there is water spray in this area, and the surrounding rock is cemented, which reduces the bearing capacity of surrounding rock and makes the roadway prone to deformation and failure.

(2) High lateral bearing pressure. Because the 11307 tail entry is close to the goaf of the 11302 working face, the pressure on the coal body is increased and the overall physical and mechanical properties are weakened, especially the stress and deformation along the goaf are more serious due to the support pressure on the side of the goaf.

(3) The pretension of the anchor rod is low. In the process of roadway support, the pretightening force of the bolt is low, which weakens the active and timely support function of the bolt, and cannot meet the requirements of roadway stability. When the surrounding rock deformation is damaged to a certain extent, the working resistance to meet the requirements can be reached, which is the main reason for the surrounding rock deformation.

## 3. Analysis of Pretightening Torque and Pretightening Force Loss Effect of Bolt Support

### 3.1. Analysis of the Relationship between Pretightening Force and Pretightening Torque of the Anchor Rod.
According to the pretightening torque applied to the bolt, the bolt

TABLE 1: 3-1 distribution of coal seam roof and floor slate.

| Rock name | Thickness (m) | Lithologic characteristics |
|---|---|---|
| Gravelly sandstone or sandy mudstone | 25.0 | Light gray, gray white, containing rock debris and mica fragments, mudstone cementation, argillaceous filling |
| Sandstone mudstone and siltstone interbedding | 1.6 | Gray siltstone and dark gray sandy mudstone, locally containing plant fossils, with parallel bedding development |
| Coal seam | 4.3 | Black dull luster, semidark briquette, containing silk charcoal, banded structure, asphalt luster, containing p yrite |
| Sandstone argillaceous | 1.5 | Dark gray sandy mudstone, locally containing plant fossils, with developed bedding |
| Sandy argillaceous and siltstone interbedding | 15.0 | Gray siltstone and dark gray sandy mudstone, locally containing plant fossils, and developed parallel bedding |
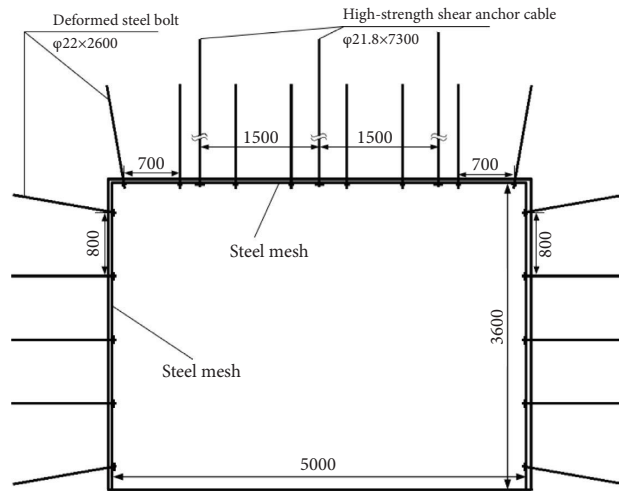
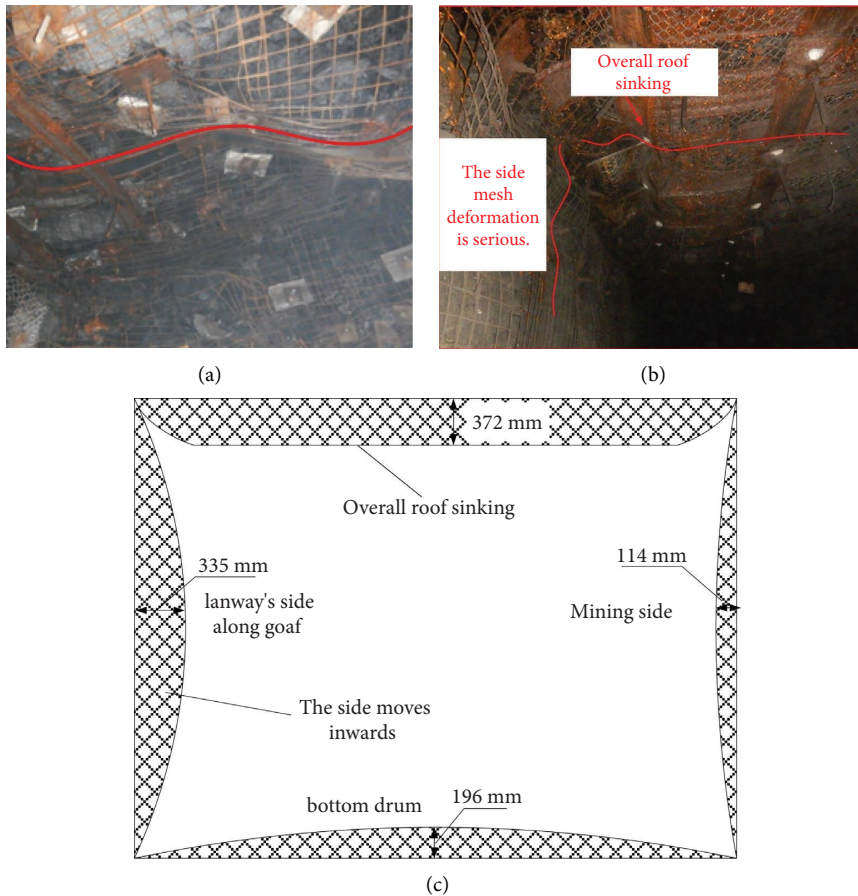FIGURE 2: 11307 section support of return airway (unit: mm).



FIGURE 3: Deformation and failure characteristics of surrounding rock. (a) Roof deformation bolt failure. (b) The overall sinking of the roof and the bulging of the side. (c) Overall deformation and failure of roadway.

produces the corresponding pretightening force, and the surrounding rock deforms under pressure and exerts pressure on the tray so as to establish the mechanical model of the bolt support structure. The nut is subjected to external torque, and its thread has an outward pull on the rod body, and there is an inward pressure on the surrounding rock through components such as trays and gaskets. The bonding force of the anchoring agent on the rod body balances the overall force of the supporting structure. Under the action of external torque, the stress of the bolt support member and the surrounding rock reaches a balance. Through the force analysis and geometric analysis of the rod body, the
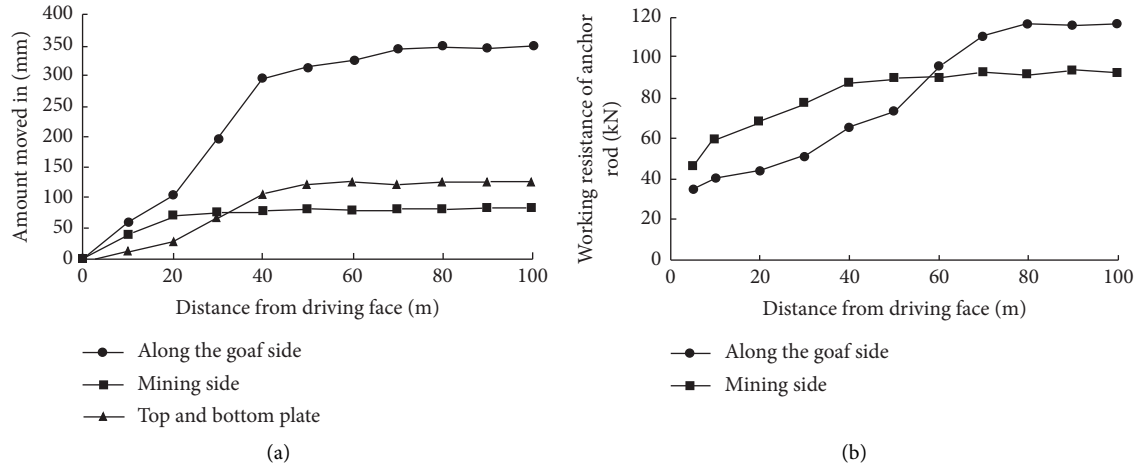
FIGURE 4: Monitoring curve of surrounding rock displacement and bolt preload during excavation. (a) Roadway displacement. (b) Working resistance monitoring of the anchor rod.

relationship between the torque applied by the bolt and the preload is obtained. The mechanical model of the bolt pretightening support member is shown in Figure 5.

$$M = \frac{2\mu_2\left(R^3 - r^3\right)\left(\cos\theta - \mu_1\sin\theta\right) + 3r\left(R^2 - r^2\right)\left(\mu_1\cos\theta + \sin\theta\right)}{3\left(R^2 - r^2\right)\left(\cos\theta - \mu_1\sin\theta\right)} T. \tag{1}$$

Let

$$\lambda = \frac{3\left(R^2 - r^2\right)\left(\cos\theta - \mu_2\sin\theta\right)}{2\mu_1\left(R^3 - r^3\right)\left(\cos\theta - \mu_2\sin\theta\right) + 3r\left(R^2 - r^2\right)\left(\mu_2\cos\theta + \sin\theta\right)}. \tag{2}$$

Therefore, the relationship between preload and preload torque is

$$T = \lambda M. \tag{3}$$

In the formula, $M$ is the preload torque. $T$ is the pretightening force of bolt. $\mu_2$ is the friction coefficient between threads. $R$ is the outer radius of the nut. $r$ is the radius of the anchor rod body. $\theta$ is the thread angle. $\mu_1$ is the friction coefficient between nut and tray. $\lambda$ is the conversion coefficient of pretightening force, which is determined by the bolt diameter, thread pitch, and friction coefficient.

According to the analysis of the abovementioned derivation formula, it can be seen that the pretightening force of the anchor rod is related to the strength of the anchor rod, the diameter of the anchor rod, the rising angle of the tail thread, the nature of the anchor body, and the friction force of each part of the component. However, the pretightening force of the anchor rod is affected by many factors. The relationship between torque and force cannot accurately

Through the analysis of the friction force between the thread, the tray, the nut, and the contact surface, the relationship between the applied external torque and the axial force of the rod body is obtained as follows:

express the actual pretightening force of the anchor rod, and there is a loss of pretightening force in the pretightening process of the anchor rod.

3.2. Bolt Pretightening Loss Analysis. The relationship between pretightening force and torque of rebar bolt in 11307 return airway is tested. The results are shown in Figure 6. F1~F3 are the pretightening force test results of the same anchor rod during multiple pretightening. However, in the field test, the pretightening force test results are still different when the same anchor rod and the pretightening torque application conditions are consistent. With the increase of the number of pretightening times, the pretightening force of the anchor rod gradually decreases.

It can be seen from the test curve that the preload force decreases gradually after repeated preload torque is applied, indicating that the repeated preload will cause preload loss. The surrounding rock contains discontinuous structural planes such as joints and fissures. During the pretightening
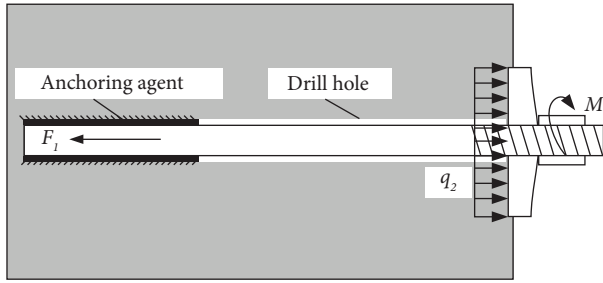
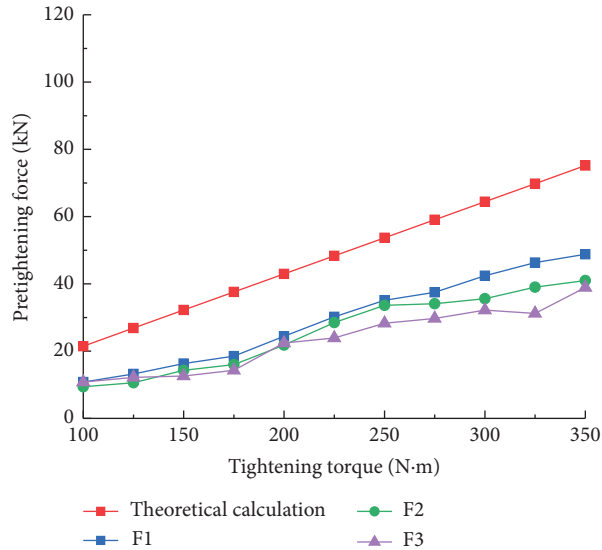FIGURE 5: Structural mechanics model of bolt pretension support.



FIGURE 6: Comparison of theoretical calculation and test results.

process, a certain pretightening torque is applied to the nut, and the tray produces pressure on the surrounding rock so that the surrounding rock is compressed and deformed, and the structural plane is pressed and closed. The surrounding rock continues to deform under the pressure of the tray, causing gaps in the contact surface between the tray and the surrounding rock, which in turn leads to a decrease in the pretightening force of the bolt.

Compared with the theoretical calculation results, there is a big difference between the measured value and the theoretical value of the bolt pretightening force, indicating that there is a pretightening force loss during the pretightening process of the bolt. By comparing the theoretical pretightening force with the measured pretightening force, the pretightening force loss and loss coefficient are calculated, and the pretightening force and pretightening torque formula are modified. The loss coefficient is the ratio of the loss to the calculated value of the preload.

$$k = \frac{T - T_0}{T}. \tag{4}$$

In the formula, $T$ is the pretightening force calculation value, $T_0$ is the measured value of preload, and $k$ is the coefficient of preload loss.

Through the analysis of the relationship between the pretightening torque and the pretightening force, it can be seen that in the actual process, the applied pretightening torque cannot be completely converted into pretightening force, and the friction between the bolt support components reduces the pretightening force. By introducing the commonly used bolt parameters, the loss caused by the bolt pretightening process is obtained. The diameters of common underground bolts are 16 mm, 18 mm, 20 mm, and 22 mm. The specific specifications of the nuts used are listed in Table 2.

The common bolt parameters with the thread angle of 5~15°, the friction coefficient between the nut and the tray 0.08~0.18, and the friction coefficient between the threads 0.05~0.15 are brought into the calculation formulas (2) and (4). The specific calculation results are shown in Table 3.

The abovementioned analysis shows that the loss of pretightening force caused by friction is inversely proportional to the diameter of the rod when the thread and working conditions of the bolt are consistent. Therefore, when the pretightening torque is the same, the selection of a larger diameter bolt will reduce the loss of bolt pretightening force. In the process of underground bolt installation, there is not only the loss caused by friction but also the influence of deformation and failure of surrounding rock [25], thus reducing the degree of tightness between surrounding rock, tray, and nut so that the bolt preload is reduced, which needs to be further determined.

## 4. Study on Loss Characteristics of Bolt Pretightening Force

*4.1. Simulation Study on Bolt Preload Loss.* A numerical simulation model of a cylinder with a diameter of 300 mm and a height of 300 mm is established, which is composed of anchor body, tray, rod body, and nut. In this model, 30 mm holes are reserved inside the model, and the tray is simplified to a plane tray of $150 \times 150 \times 10$ mm, with a tray hole of 28 mm, as shown in Figure 7. One end of the anchor body is preloaded by nuts and trays, and the other end is fixed to the boundary.

ABAQUS is used to establish a three-dimensional spatial node model. The length, load, mass, time, and stress measurement units in the model are mm, N, Ton, S, and MPa, respectively. The anchorage specimen, bolt, and tray are all created in the part module by using the 8-node hexahedron-reduced integral solid element, and the anchorage body specimen, bolt rod body, bolt nut, and tray member are created by stretching and moving methods. The property module defines component properties. The elastic modulus of nuts, trays, and rods is $2.1 \times 10^5$ MPa, and the Poisson's ratio is 0.25. The joint between the anchored solid specimen and the bottom of the rod body is completely fixed in all translational degrees of freedom, and the boundary conditions begin to play a role in the initial analysis step. At the same time, in order to prevent the rod body from being affected by the rotation of the nut, the joint of the cylindrical surface of the rod body is limited in the rotational degree of freedom. The finite element model adopts the static analysis

TABLE 2: Nut specifications.

| Bolt diameter (mm) | Nut outer diameter $R$ (mm) | Nut inner diameter $r$ (mm) |
|---|---|---|
| 16 | 19 | 8 |
| 18 | 20 | 9 |
| 20 | 21 | 10 |
| 22 | 24 | 11 |

TABLE 3: Pretightening force coefficients of different diameters.

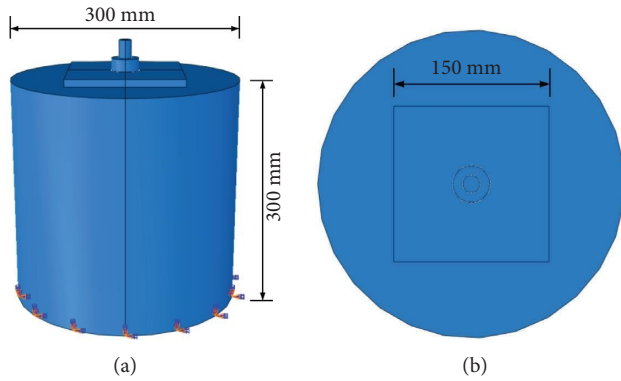| Bolt diameter (mm) | Theoretical coefficients ($\lambda_1$) | The coefficient after loss ($\lambda_2$) | The proportion of loss |
|---|---|---|---|
| 16 | 0.23~0.71 | 0.14~0.37 | 0.39~0.48 |
| 18 | 0.21~0.64 | 0.12~0.34 | 0.43~0.47 |
| 20 | 0.19~0.57 | 0.11~0.31 | 0.42~0.45 |
| 22 | 0.17~0.52 | 0.10~0.28 | 0.41~0.46 |



FIGURE 7: Numerical simulation model diagram. (a) Front view. (b) Vertical view.

mode, and the analysis step setting program is " static, general." By setting the constraint point in the interaction, the outer surface of the coupling nut is set, and the load is applied to the constraint point by setting the torque, and the value is 350000 N·mm.

In order to study the influence of rod diameter and thread pitch on the pretightening force of the anchor rod, the anchor rods with common rod diameters of 18 mm, 20 mm, and 22 mm and thread pitch parameters of 2 mm, 4 mm, 6 mm, and 8 mm were selected for combination and classification, and the relationship between pretightening force and pretightening torque of different specifications of the anchor rod was simulated.

The simulation results are shown in Figures 8~10:

As shown in Figure 11, the results show that the loss of bolt pretightening force is linearly related to the pretightening torque and inversely proportional to the bolt diameter and thread pitch. With the increase of bolt diameter or pitch, the bolt pretightening force decreases gradually and the loss of pretightening force decreases gradually.

### 4.2. Field Test of Pretightening Loss of Bolt Support

*4.2.1. Test Area Selection and Test Instruments.* In order to obtain the loss of bolt pretightening force caused by surrounding rock deformation, the roadway side of 11307 return air roadway was tested. As shown in Figure 12, the SATA (SATA)3/4″G series preset torsion wrench 100 N·m–550 N·m, MCS-400 mine intrinsically safe anchor dynamometer is selected.

*4.2.2. Analysis of Field Test Results.* The diameter of the thread steel fine wire anchor rod is 22 mm, the height of the longitudinal rib of the rod is 0.85 mm, the spacing is 12 mm, the length is 2600 mm, the thread length is 300 mm, and the pitch is about 3 mm. The relationship between the pretightening force and the pretightening torque of the bolt is shown in Table 4, and the results are shown in Figure 13.

The parameters of the screw steel wire anchor are brought into the formula (2): $\mu_1 = 0.12$, $\mu_2 = 0.15$, $R = 0.024$ m, $r = 0.011$ m, and $\theta = 2.5°$ to calculate the theoretical value of the pretightening force of the anchor. Comparing the test results, the pretightening force loss of the bolt is calculated, as shown in Figure 14, and the specific calculation results are listed in Table 5.

In the actual pretightening process, the loss of threaded steel thin wire anchor rod is linearly related to the pretightening torque. With the increase of pretightening torque, the loss of anchor rod pretightening force increases gradually. By comparing with the theoretical calculation results, the bolt preload loss coefficient is calculated, and the results are shown in Figure 15.

The pretightening force loss coefficient is 0.19~0.43. According to the test of the physical and mechanical properties of the surrounding rock in the previous study, the elastic modulus of the surrounding rock is 1367 MPa, which is basically consistent with the pretightening force loss coefficient obtained from the indoor test and numerical simulation results.

## 5. Engineering Application

*5.1. Bolt Pretightening Support Design.* After obtaining the relationship between the actual bolt pretightening torque and the pretightening force, it is necessary to determine the reasonable pretightening force in the field application
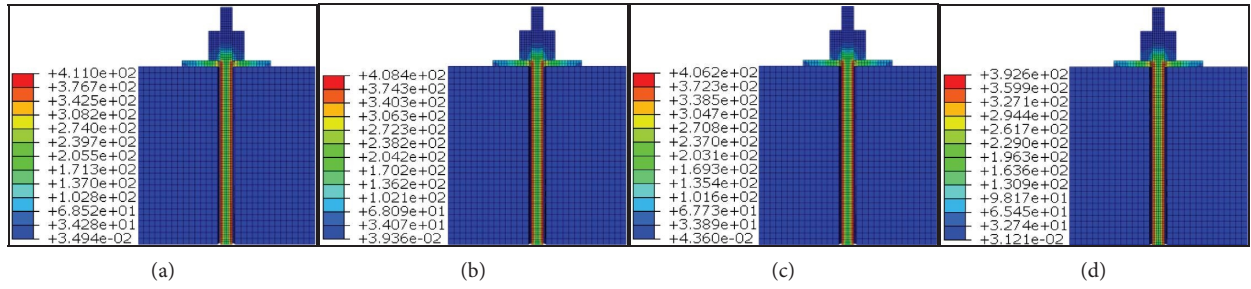
FIGURE 8: Results of 20 mm bolt with different pitches. (a) Pitch: 2 mm. (b) Pitch: 4 mm. (c) Pitch: 6 mm. (d) Pitch: 8 mm.
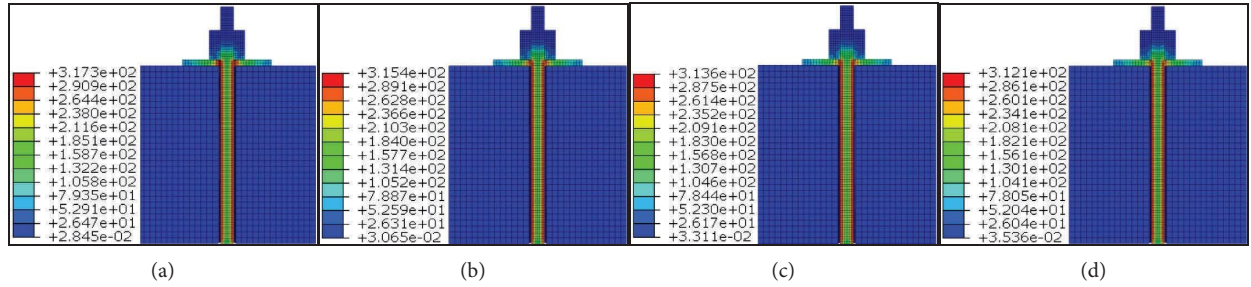


FIGURE 9: Results of 22 mm bolt with different pitches. (a) Pitch: 2 mm. (b) Pitch: 4 mm. (c) Pitch: 6 mm. (d) Pitch: 8 mm.
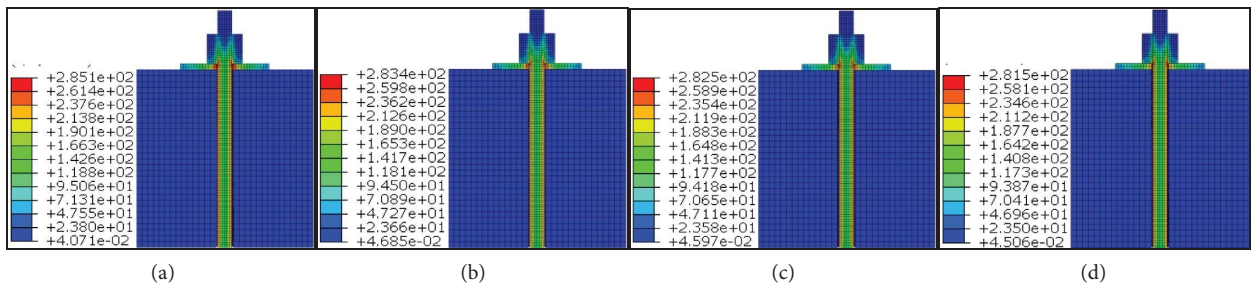


FIGURE 10: Results of 25 mm bolt with different pitches. (a) Pitch: 2 mm. (b) Pitch: 4 mm. (c) Pitch: 6 mm. (d) Pitch: 8 mm.
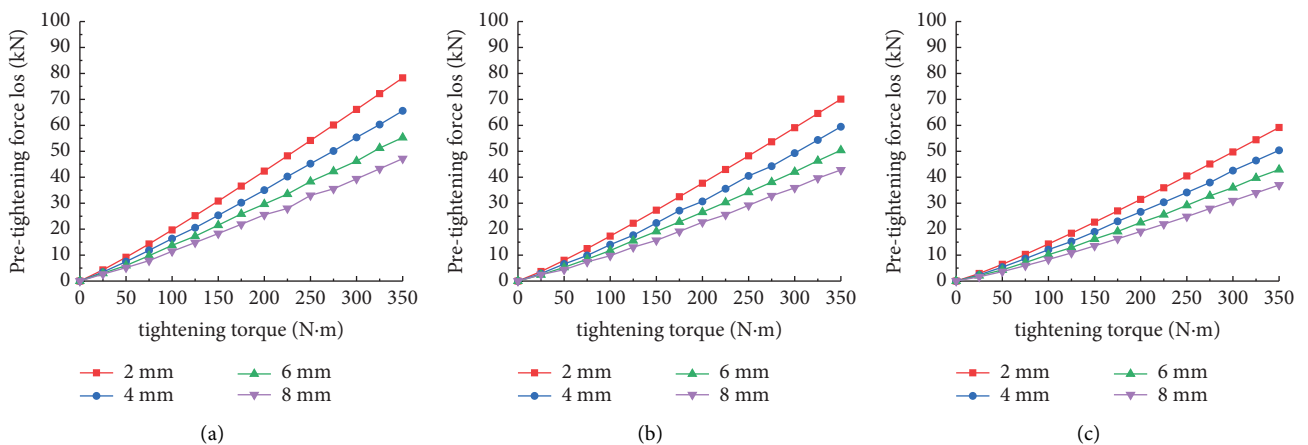


FIGURE 11: Curve of bolt pretension force loss. (a) Diameter: 20 mm. (b) Diameter: 22 mm. (c) Diameter: 25 mm.

process so as to apply the corresponding pretightening torque. The design pretightening force of the bolt should be greater than 60 kN. According to the relationship between the modified pretightening torque and the pretightening force, when the pretightening force reaches 60 kN, the pretightening torque is 300 N·m.
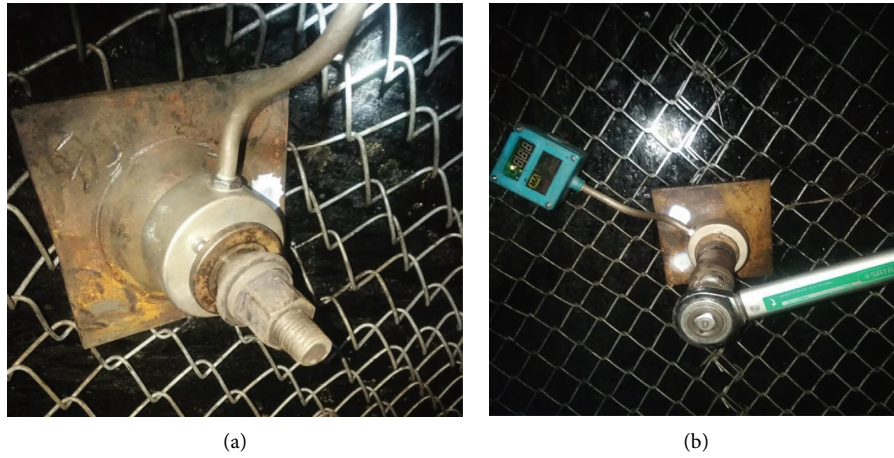
(a)



(b)

FIGURE 12: Preload test process. (a) Dynamometer installation. (b) Preload and preload torque test.

TABLE 4: Test results of the ribbed steel wire anchor rod.

| Tightening torque (Nm) | Bolt preload (kN) | | | | | | |
|---|---|---|---|---|---|---|---|
| | 1 | 2 | 3 | 4 | 5 | 6 | 7 |
| 100 | 23.40 | 29.20 | 23.40 | 22.90 | 23.90 | 20.00 | 27.30 |
| 125 | 28.80 | 33.20 | 30.20 | 27.30 | 29.70 | 24.90 | 32.20 |
| 150 | 31.70 | 38.00 | 35.10 | 31.70 | 34.10 | 27.80 | 40.00 |
| 175 | 32.20 | 44.90 | 40.00 | 32.20 | 36.60 | 32.20 | 43.90 |
| 200 | 41.50 | 51.20 | 45.40 | 39.50 | 43.40 | 41.50 | 48.80 |
| 225 | 46.30 | 56.10 | 50.20 | 46.30 | 44.40 | 44.90 | 53.20 |
| 250 | 46.30 | 61.00 | 51.20 | 52.70 | 51.20 | 49.30 | 55.60 |
| 275 | 51.70 | 65.40 | 54.10 | 51.20 | 57.10 | 53.20 | 58.10 |
| 300 | 61.00 | 70.80 | 57.60 | 51.60 | 63.90 | 58.10 | 60.50 |
| 325 | 64.40 | 78.10 | 61.00 | 63.90 | 67.60 | 64.40 | 62.90 |
| 350 | 72.70 | 79.50 | 65.90 | 70.80 | 69.30 | 68.80 | 65.90 |
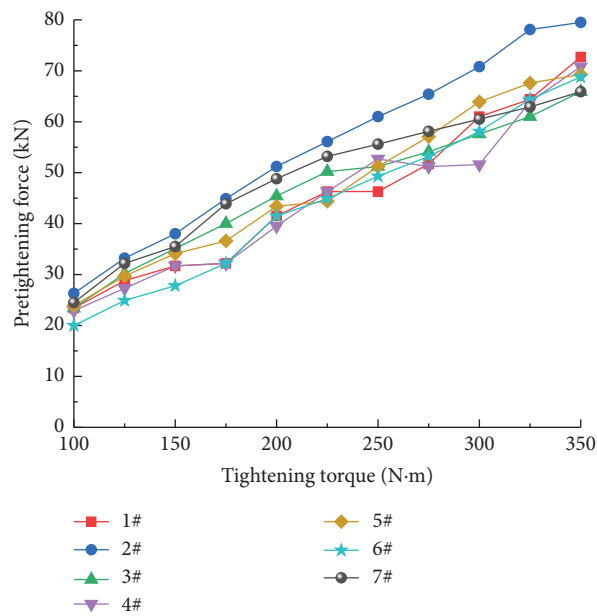


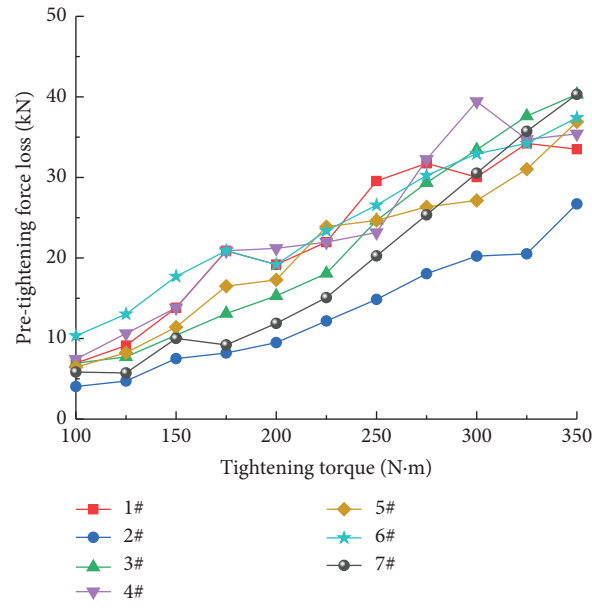FIGURE 13: Test results of threaded steel fine wire bolt.

Figure 14: Relationship between pretension force loss and moment of pretension of threaded steel fine wire bolt.

Table 5: Calculation of pretightening force and loss of thread steel fine wire bolt.

| Tightening torque (Nm) | Theoretical value (kN) | Pretightening force loss (kN) | | | | | | |
| --- | --- | --- | --- | --- | --- | --- | --- | --- |
| | | 1# | 2# | 3# | 4# | 5# | 6# | 7# |
| 100 | 30.34 | 6.94 | 4.04 | 6.94 | 7.44 | 6.44 | 10.34 | 5.84 |
| 125 | 37.93 | 9.13 | 4.73 | 7.73 | 10.63 | 8.23 | 13.03 | 5.73 |
| 150 | 45.52 | 13.82 | 7.52 | 10.42 | 13.82 | 11.42 | 17.72 | 10.02 |
| 175 | 53.10 | 20.90 | 8.20 | 13.10 | 20.90 | 16.50 | 20.90 | 9.20 |
| 200 | 60.69 | 19.19 | 9.49 | 15.29 | 21.19 | 17.29 | 19.19 | 11.89 |
| 225 | 68.28 | 21.98 | 12.18 | 18.08 | 21.98 | 23.88 | 23.38 | 15.08 |
| 250 | 75.86 | 29.56 | 14.86 | 24.66 | 23.16 | 24.66 | 26.56 | 20.26 |
| 275 | 83.45 | 31.75 | 18.05 | 29.35 | 32.25 | 26.35 | 30.25 | 25.35 |
| 300 | 91.03 | 30.03 | 20.23 | 33.43 | 39.43 | 27.13 | 32.93 | 30.53 |
| 325 | 98.62 | 34.22 | 20.52 | 37.62 | 34.72 | 31.02 | 34.22 | 35.72 |
| 350 | 106.21 | 33.51 | 26.71 | 40.31 | 35.41 | 36.91 | 37.41 | 40.31 |
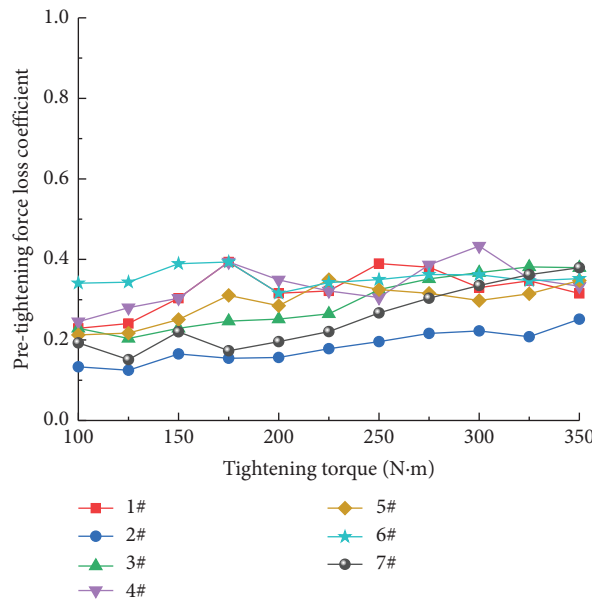


Figure 15: Relationship between pretension force coefficient and moment of pretension.
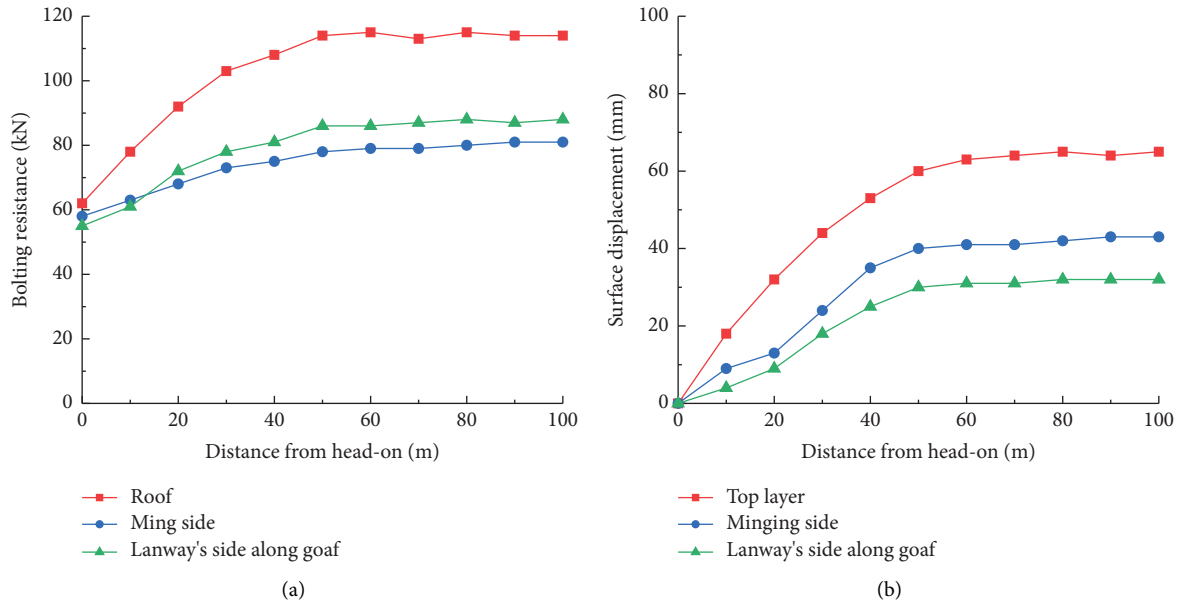
FIGURE 16: Application area preload monitoring. (a) Monitoring of bolt working resistance. (b) Monitoring displacement of roadways.
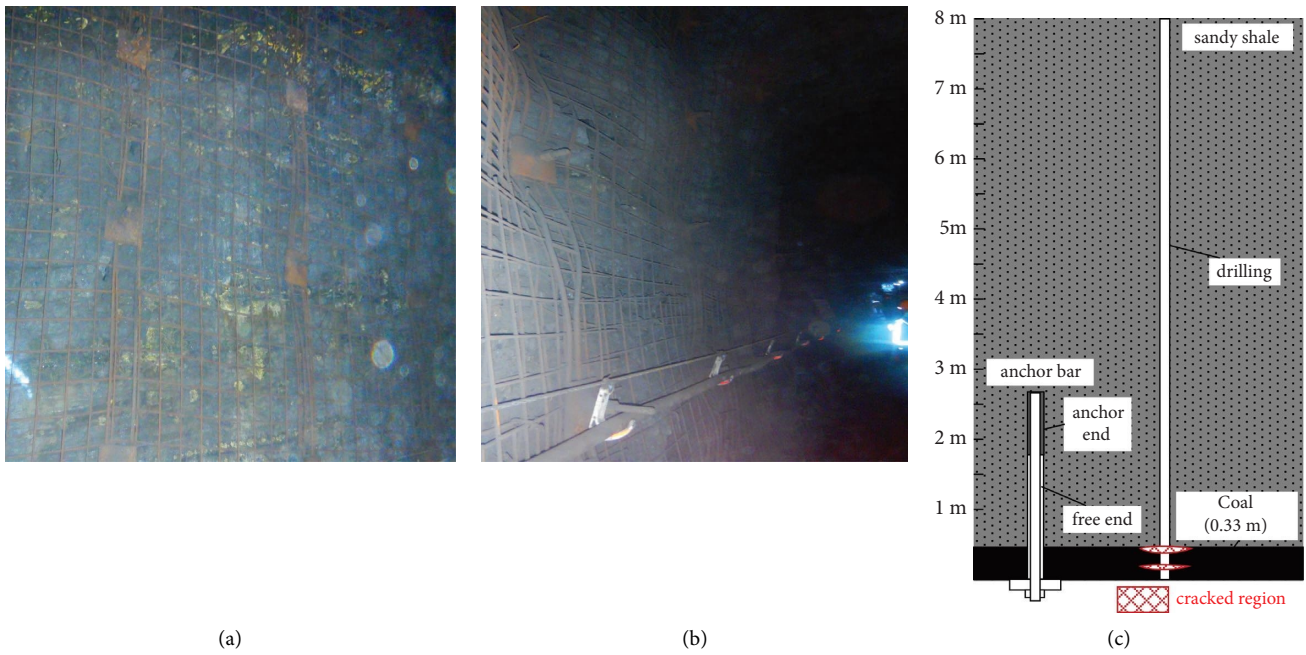


FIGURE 17: Application area effect. (a) Mining side. (b) Lanway's side along goaf. (c) Surrounding rock fracture diagram.

*5.2. Application Effect.* The designed pretightening torque is applied on the heading face of 11307 return air roadway, and the working resistance of bolt and roadway deformation are monitored, as shown in Figure 16.

After the pretightening torque is adjusted to 300 Nm, the pretightening force of the bolt is about 60 kN. As the working face advances, the force rises faster. When the roadway is excavated for 30~40 m, the bolt support resistance of the two sides tends to be stable, which is 78~115 kN. The deformation of the surrounding rock tends

to be stable, and there is no obvious continuous increase. During the excavation of the roadway, the displacement of the roof and floor is 34 mm, the displacement of the gob side is 80 mm, and the displacement of the mining side is 52 mm.

As shown in Figure 17, after the actual pretightening force of the bolt is increased, the overall resistance to deformation and failure of the surrounding rock is improved. From the control effect, the overall deformation of the roadway is small, and the stability of the roadway is effectively controlled.

## 6. Main Results

(1) By investigating the deformation and failure characteristics of 11307 return air roadway after excavation, it is found that the deformation of surrounding rock is large and the deformation speed is fast, and the fracture of surrounding rock is mainly distributed in the free section of bolt. By analyzing the influencing factors of roadway deformation and failure, it is found that the actual pretightening force of bolt is low, only 16∼23 kN, which is lower than the design pretightening force of bolt, and it is one of the key factors causing the deformation and failure of surrounding rock.

(2) By analyzing the stress characteristics in the process of bolt pretightening, the mechanical model of bolt pretightening structure is established. From the aspects of force balance and moment balance of each component, the relationship between bolt pretightening force and pretightening torque is derived. The influence law of bolt pretightening force is analyzed. The difference between the theoretical value and the measured value of pretightening force is compared. The loss coefficient $k$ of pretightening force is proposed and the relationship is modified. Through the indoor, numerical simulation test and field test, the relationship between pretightening force and pretightening torque of bolt is tested. Compared with the calculation results of theoretical derivation formula, the loss coefficient of pretightening force of bolt will increase by 0.03∼0.07 for every 2 mm increase of thread pitch of bolt body. Combined with the field test, the relationship between pretightening torque and pretightening force is corrected, and the loss coefficient of pretightening force caused by surrounding rock is calculated to be 0.19∼0.43.

(3) Based on the design method of bolt pretightening support, the bolt pretightening force is not less than 60 kN. Combined with the relationship between bolt pretightening force and pretightening torque, the pretightening torque is not less than 275 N·m. In the field application, the pretightening torque is 300 Nm, the pretightening force of the bolt is about 60 kN, and the loss coefficient of the pretightening force is 0.3, which is in line with the modified relationship between the pretightening force and the pretightening torque for field application. The results show that the optimized design pretightening torque can significantly reduce the deformation of the roadway side, the support effect is significantly improved, and the stability of the surrounding rock is effectively controlled.

## Data Availability

The data used to support the findings of this study are available from the corresponding author upon request.

## Conflicts of Interest

The authors declare that they have no conflicts of interest.

## Authors' Contributions

F.Y., T.Z., D.Z., and X.Z. contributed to the methodology; F.Y. validated the study; F.Y., T.Z., and X.Z. contributed to formal analysis; B.S. contributed to investigation, writing the original draft, and reviewing and editing; T.Z., D.Z., and P.F. contributed to resources; P.F. and D.Z. contributed to data curation. All the authors have read and agreed to the published version of the manuscript.

## Acknowledgments

## References

[1] Q. B. Meng, L. J. Han, W. G. Qiao, D. G. Lin, and J. D. Fan, "Evolution of surrounding rock in pioneering roadway with very weakly cemented strata through monitoring and analysising," *Journal of China Coal Society*, vol. 38, no. 4, pp. 572–579, 2013.

[2] P. Wang, B. S. Zhang, L. Wang, X. Y. Lin, X. F. Song, and J. Q. Guo, "Research on roof falling mechanism and support technology of mining roadway in expansive soft rock," *Journal of Mining and Strata Control Engineering*, vol. 2, no. 2, pp. 53–61, 2020.

[3] L. H. Sun, H. G. Ji, and B. S. Yang, "Physical and mechanical characteristic of rocks with weakly cemented strata in Western representative mining area," *Journal of China Coal Society*, vol. 44, no. 3, pp. 866–874, 2019.

[4] Y. Sun, G. Li, J. Zhang, and J. Xu, "Failure mechanisms of rheological coal roadway," *Sustainability*, vol. 12, no. 7, p. 2885, 2020.

[5] H. P. Kang, "Study and application of complete rock bolting technology to coal roadway," *Chinese Journal of Rock Mechanics and Engineering*, vol. 24, no. 21, pp. 3959–3946, 2005.

[6] L. X. Chen, W. Y. Guo, D. X. Zhang, and T. B. Zhao, "Experimental study on the influence of prefabricated fissure size on the directional propagation law of rock type-I crack," *International Journal of Rock Mechanics and Mining Sciences*, vol. 160, Article ID 105274, 2022.

[7] H. P. Kang, "Development and prospects of support and reinforcement materials for coal mine roadways," *Coal Science and Technology*, vol. 49, no. 4, pp. 1–11, 2021.

[8] H. P. Kang, J. Lin, and Y. Z. Wu, "Mechanical performances and compatibility of rock bolt components," *Journal of China Coal Society*, vol. 40, no. 1, pp. 11–23, 2015.

[9] N. Zhang, J. G. Kan, and S. Yang, "Control technology and failure types of anchor bolt support and U-steel frame support," *Coal Science and Technology*, vol. 43, no. 6, pp. 41–47, 2015.

[10] N. Zhang, G. C. Li, and J. G. Kan, "Influence of soft interlayer location in coal roof on stability of roadway bolting structure," *Rock and Soil Mechanics*, vol. 32, no. 9, pp. 2753–2758, 2011.

[11] Y. L. Tan, F. H. Yu, C. F. Ma, G. S. Zhang, and W. Zhao, "Research on collabration control method of bolt/cable-surrounding rock deformation in coal roadway with weakly cemented soft rock," *Coal Science and Technology*, vol. 49, no. 1, pp. 198–207, 2021.

[12] C. J. Hou and H. L. Guo, "Orientation of technical development of rockbolting in in-seam gateways in China," *Journal of China Coal Society*, no. 2, pp. 113–118, 1996.

[13] W. Wang, Y. S. Pan, and Y. H. Xiao, "Synergistic resin anchoring technology of rebar bolts in coal mine roadways," *International Journal of Rock Mechanics and Mining Sciences*, vol. 151, Article ID 105034, 2022.

[14] Y. H. Cao and Y. T. Li, "Deformation control of surrounding rocks of mining roadway in deep and close lower coal seam," *Coal Science and Technology*, vol. 49, no. 9, pp. 76–81, 2021.

[15] H. P. Kang, T. M. Jiang, and F. Q. Gao, "Effect of pretensioned stress to rock bolting," *Journal of China Coal Society*, vol. 32, no. 7, pp. 680–685, 2007.

[16] H. P. Kang, "Seventy years development and prospects of strata control technologies for coal mine roadways in China," *Chinese Journal of Rock Mechanics and Engineering*, vol. 40, no. 1, pp. 1–30, 2021.

[17] J. L. Hou, C. N. Li, and N. Zhao, "Key technology and application of pre-stressed anchor to improve pretightening force," *Coal Science and Technology*, vol. 50, no. 12, pp. 1–13, 2022.

[18] S. J. Wei and P. F. Gou, "Analogy simulation test on strengthening effect for pretention of bolts on anchorage body," *Journal of China Coal Society*, vol. 37, no. 12, pp. 1987–1993, 2012.

[19] J. K. Long and Y. T. Liu, "Experiment study of synergistic anchorage efficiency in anchorage body with preload bolt," *Chinese Journal of Rock Mechanics and Engineering*, vol. 35, no. 1, pp. 2795–2802, 2016.

[20] J. Q. Jia, W. F. Zheng, and G. Z. Chen, "Numerical analysis of prestressed anchor flexible retaining method," *Chinese Journal of Rock Mechanics and Engineering*, vol. 24, no. 21, pp. 3978–3982, 2005.

[21] J. L. Cai, M. Tu, and H. L. Zhang, "Deformation and instability mechanism and control technology of mining gateway for Jurassic weak-cemented soft rock roadways," *Journal of Mining & Safety Engineering*, vol. 37, no. 6, pp. 1114–1122, 2020.

[22] W. Y. Guo, L. X. Chen, L. M. Yin et al., "Experimental study on the influence of loading rate on the directional propagation law of rock mode-I cracks," *Theoretical and Applied Fracture Mechanics*, vol. 125, Article ID 103873, 2023.

[23] E. Unal, I. Ozkan, and G. Cakmakci, "Modeling the behavior of longwall coal mine gate roadways subjected to dynamic loading," *International Journal of Rock Mechanics and Mining Sciences*, vol. 38, no. 2, pp. 181–197, 2001.

[24] A. Hyett, W. Bawden, and R. Reichert, "The effect of rock mass confinement on the bond strength of fully grouted cable bolts," *International Journal of Rock Mechanics and Mining Sciences & Geomechanics Abstracts*, vol. 29, no. 5, pp. 503–524, 1992.

[25] H. P. Kang, J. Lin, and M. J. Fan, "Investigation on support pattern of a coal mine roadway within soft rocks—a case study," *International Journal of Coal Geology*, vol. 140, pp. 31–40, 2015.

[26] W. Ru, S. Hu, J. Ning et al., "Study on the rheological failure mechanism of weakly cemented soft rock roadway during the mining of close-distance coal seams: a case study," *Advances in Civil Engineering*, vol. 2020, Article ID 8885849, 20 pages, 2020.

[27] K. Zhang, G. Zhang, R. Hou, Y. Wu, and H. Zhou, "Stress evolution in roadway rock bolts during mining in a fully mechanized longwall face, and an evaluation of rock bolt support design," *Rock Mechanics and Rock Engineering*, vol. 48, no. 1, pp. 333–344, 2015.

[28] C. Wang, Z. S. Du, and Z. B. Li, "Calculation and prediction of initial support pressure in bolt support," *Journal of China Coal Society*, vol. 37, no. 12, pp. 1982–1986, 2012.

[29] Z. B. Li, N. Zhang, and C. L. Han, "Relationship between pretightening force and tightening torque," *Journal of China University of Mining & Technology*, vol. 41, no. 3, pp. 189–193, 2012.

[30] J. G. Guo and Y. T. Liu, "Experiment study on bolt and accessories affected to conversion performances of pretension," *Coal Science and Technology*, vol. 45, no. 1, pp. 142–147, 2017.

[31] Y. K. Fu, "Influence factors of interconversion between pretightening force and tightening torque," *Journal of Mining & Safety Engineering*, vol. 33, no. 5, pp. 800–805, 2016.

[32] Q. Wang and Y. Z. Wu, "Study on bolt pre-tension control in underground mine," *Coal Science and Technology*, vol. 38, no. 4, pp. 572–579, 2011.

[33] P. Cheng, H. P. Kang, and W. J. Ju, "Experimental study on mechanical properties of thread end of rock bolts," *Journal of China Coal Society*, vol. 38, no. 11, pp. 1929–1933, 2013.

[34] L. X. Chen, W. Y. Guo, Y. J. Jiang et al., "Experimental study on influence of lithology on directional propagation law of type-I cracks," *Journal of Central South University*, vol. 30, no. 10, pp. 3322–3334, 2023.

[35] B. Nadi, O. Tavasoli, D. P. N. Kontoni, and A. Tadayon, "Investigation of rock slope stability under pore-water pressure and structural anisotropy by the discrete element method," *Geomechanics and Geoengineering*, vol. 16, no. 6, pp. 452–464, 2019.

[36] O. Tavasoli, A. Mokhtarpour, A. Asakereh, and A. Pishkari, "Numerical Investigation on the effect of the internal water pressure and leakage force on the behavior of tunnel lining," *Journal of Dam and Hydroelectric Powerplant*, vol. 6, no. 23, pp. 1–12, 2020.

[37] B. Nadi, O. Tavasoli, P. K. Esfeh, and D. P. N. Kontoni, "Characteristics of spatial variability of shear wave velocity on seismic response of slopes," *Arabian Journal of Geosciences*, vol. 13, no. 16, pp. 800–812, 2020.

[38] Y. Tian, H. Qian, Z. Cao, D. Zhang, and D. Jiang, "Identification of pre-tightening torque dependent parameters for empirical modeling of bolted joints," *Applied Sciences*, vol. 11, no. 19, p. 9134, 2021.

[39] N. Afzali, N. Stranghöner, J. Pilhagen, T. Manninen, and E. Schedin, "Viscoplastic deformation behaviour of preloaded stainless steel connections," *Journal of Constructional Steel Research*, vol. 152, pp. 225–234, 2019.